

# The Relationship between the Shape of Backface Deformation and Behind-Armour Blunt Trauma

K. A. Rafaels<sup>1</sup>, M. E. Lizins<sup>2</sup>, K. L. Loftis<sup>3</sup>, and C. A. Bir<sup>4</sup>

<sup>1</sup>*Army Futures Command, CCDC Army Research Laboratory, Aberdeen Proving Ground, MD, USA, karin.a.rafaels.civ@mail.mil*

<sup>2</sup>*College Qualified Leaders Program, Army Futures Command, CCDC Army Research Laboratory, Aberdeen Proving Ground, MD, USA*

<sup>3</sup>*Army Futures Command, CCDC, DAC, Aberdeen Proving Ground, MD, USA*

<sup>4</sup>*Department Chair of Biomedical Engineering, Wayne State University, Detroit, MI, USA*

**Abstract.** Measuring the imprint of body armour backface deformation in clay is still the most widely-used method to assess BABT. Previous efforts have demonstrated that the current metric using the maximum depth in clay may not predict injuries as well as a metric containing the velocity of the armour backface deformation; however, measuring the velocity requires upgrading facilities with expensive equipment and, even then, backface velocity is difficult to capture. This study investigates the association of thoracic injury with the depth and shape of the backface deformation in clay that is associated with the energy and energy density of the impact. This metric including depth and shape reflects the empirical evidence that deeper deformations are more likely to cause injury; but for similar depths, deformations with larger volumes are more injurious. Reconstructions of several law enforcement survivor cases of behind-armour blunt trauma to the chest were performed to obtain the backface signature in clay for these known injury events. Moulds were made of the backface signatures and then scanned to characterise the diameter, depth, volume, and surface area of the deformations. The relationship between the depth and surface area/volume ratio and the injuries from the survivor cases were determined. The depth and surface area/volume ratio showed good correlation to the injury severities reported in the survivor cases. The analysis also confirmed that even if the surface area to volume ratio between two different backface deformations were maintained, the impact that results in a deeper clay depth has a higher risk of increased injury severity. The dataset for this analysis is currently limited, but the relationship exhibits potential for an improved metric that can be easily implemented into current testing methodologies and facilities.

## 1. INTRODUCTION

Although many factors of the backface deformation (BFD) of body armour can contribute to injury risk, it is not feasible in the near-term to define a universal and all-encompassing injury assessment tool for behind-armour blunt trauma (BABT) since there are far too many potential locations and angles of impacts, mechanisms of thoracic injury, and various threats and protection systems that change the signature of the BFD. Therefore, simple metrics have been implemented to evaluate BABT injury risk. One of the most common metrics involves the evaluation of the BFD of the armour imprinted into a clay medium, such as in the NIJ 0101.06 standard [1]. Previous efforts have demonstrated that the current metric using the maximum depth in clay may not predict injuries as well as a metric containing the velocity of the armour backface deformation [2]. However, it is difficult to measure backface velocity. Common current techniques to measure the backface velocity of armour include: digital image correlation and tracking of unbacked armour [3-4], flash x-ray images of the armour on the backing material [5-8], high-speed video tracking and analysis of gelatin-backed armour [9-11], and inner surface measurements of thoracic rig membranes [12-14]. Each technique helps in the understanding of the backface armour response, but all have limitations. For example, unbacked armour does not demonstrate the same ballistic performance as backed armour, current flash x-ray technology has limited spatial and/or temporal resolution, high-speed video tracking is difficult to implement with hard plates that have curvature in more than one plane, and the thoracic rig membranes act as mechanical filters of the backface signature (BFS). Furthermore, these techniques to measure velocity are not commonly found in certification labs, and would add significant costs to implement. Consequently, a metric that can be determined with minimal alteration of the current clay methodology that is better correlated to injury than clay depth would be desirable to address the immediate need to evaluate newer and lighter-weight armour systems.

Previous work has investigated the relationship of the volume of the displaced clay with increased severity of injury, but it was not shown to be as well correlated as depth [2]. Even though the volume of displaced clay should be correlated to the amount of energy imparted to the body during ballistic events, the way in which that energy is deposited also affects the injury risk, e.g., the contact area and

sharpness of the impact [15-18]. The impression left in the clay can only provide the greatest extent of the deformation and not the evolution of the contact area over the duration of the behind-armour event. Using the area of the top of the crater (in the same plane as the original clay surface) does not adequately represent the changes in contact area against the body during the entire BABT impact event. Following the association of penetrator geometry with injury risk [17-18], then if the geometry of the backface is sharper, then the force required to penetrate soft tissue would be decreased. Ideally, all of the clay deformations would be simple, spherical geometries, so the sharpness would be calculated by obtaining the inverse of the radius of curvature at the bottom of the crater. However, it is not only the radius of curvature that affects the injury risk. For example, deformations with the same radius of curvature can have different geometries (Figure 1a) with potentially different injury risks, such as increases in volume of displaced clay. Furthermore, the geometry of the deformation can be irregular such that the radius of curvature is not the same along the bottom surface of the crater (Figure 1b). To quantify the effect of the geometry of the deformation, a surface area/volume ratio (SA/V) of the deformation was calculated since for similar depths, radii of curvature, or crater diameter, a larger surface area to volume ratio would indicate an impact with a smaller contact area.

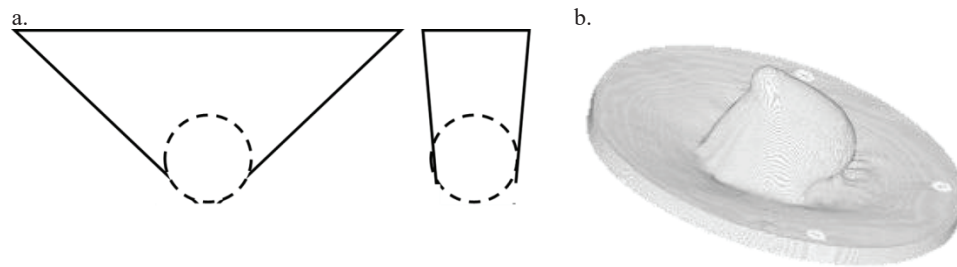


**Figure 1.** a. Examples of deformations with identical radii of curvature, but different crater geometries. b. An example of a deformation with an irregular geometry.

Measuring the BFS in clay is still a widely-used method to assess BABT. Despite clay depth having been shown to have only a moderate correlation to increased injury severity [2], it is still the only official metric used to assess BABT. Hence, an examination into alternative metrics that can be used with minimal modification to the clay methodology, and inclusion of parameters associated with injury risks may allow for a more immediate improvement of a test methodology to assess and/or certify the performance of body armour. Examining injuries from reconstructed cases of BABT events on clay, the relationship between depth and SA/V and the injuries from the cases will be determined.

## 2. METHODOLOGY

This study expanded on previous efforts to obtain and re-create cases of BABT on Roma Plastilina No. 1 clay [2, 19-20]. Similar to the study investigating the association of other clay metrics with the reconstructed cases of BABT, only handgun round impacts to the chest, defined as impact locations over the sternum or rib cage, were considered in this investigation. When available, the data previously collected in [20] was re-evaluated for this study. Additional re-creations were performed on newly-acquired cases, or for previously obtained cases if the case did not have a mould of the clay depression available, and if exemplar armour panels were available to do so. Ultimately, there were a total of 20 cases included in this analysis.

The new re-creations were performed in a similar manner to the ones previously described [20]. Prior to any data collection, approval was garnered from the Wayne State University Human Investigation Committee (HIC) and/or the University of Southern California Office for the Protection of Research Subjects (OPRS) Institutional Review Board (IRB). In summary, through surveys, interviews, medical reports, and police reports, details regarding the armour, firearm, ammunition, and range were obtained. Each incident was then re-created using the reported munition, distance, impact location, and either the same or equivalent armour system, verified by the manufacturer. Some specifics are provided in Table 1. The armour was tested on Roma Plastilina No. 1 clay conditioned in the same manner as outlined in the NIJ standard [1]. The armour was strapped to the clay with 51 mm (2-in.) wide straps, ensuring that the intended impact location was at least 76 mm (3-in.) from the border of the clay box or

any of the calibration indentations. Since the obliquity of the shotline was not well characterised in the collected data, all tests were performed with a 0° obliquity.

**Table 1.** Summary of law enforcement BABT cases

| Case            | Threat Caliber | Threat Type | Threat Weight (gr) | Range (m) | Armour Level (NIJ) | Armour Description                          |
|-----------------|----------------|-------------|--------------------|-----------|--------------------|---|
| NM07^<br>ribs'  | .45            | JHP         | 230                | 1.8       | IIIA               | Aramid/UHMWPE                               |
| 990             | .40 S&W        | FMJ         | 180                | 2.4       | II                 | Aramid                                      |
| 3029            | .357 Mag       | JHP         | 110                | 4.6       | II                 | Aramid                                      |
| 3138            | .40 S&W        | JHP         | 135                | 0.3       | IIIA               | Aramid                                      |
| 1805            | .357 Mag       | FMJ FN      | 158                | 0.3       | II                 | Aramid                                      |
| 1753            | 9 mm           | FMJ         | 124                | 2.4       | II                 | Aramid                                      |
| 3123            | .38 Sp         | FMJ         | 158                | 1.5       | II                 | Aramid/UHMWPE                               |
| 2576            | 9 mm           | JHP         | 115                | 1.8       | II                 | Aramid/UHMWPE                               |
| 2840'           | 9 mm           | JHP         | 147                | 3.0       | II                 | Aramid/UHMWPE<br>w/aramid-based trauma pack |
| 3128            | 9 mm           | FMJ         | 124                | 0.6       | II                 | Aramid                                      |
| 1716            | .38 Sp         | FMJ FN      | 158                | 0.9       | IIIA               | Aramid/UHMWPE                               |
| 3166            | 9 mm           | JHP         | 147                | 1.8       | IIIA               | Aramid/UHMWPE                               |
| NM07^<br>chest' | .45            | JHP         | 230                | 1.8       | IIIA               | Aramid/UHMWPE<br>w/aramid-based trauma pack |
| 3109'           | .45            | FMJ         | 230                | 0.3       | IIIA               | Aramid                                      |
| 2914'           | .380           | FMJ         | 90                 | 2.4       | II                 | Aramid/UHMWPE                               |
| 3167'           | .45            | FMJ         | 230                | 1.4       | IIIA               | Aramid                                      |
| 3108'           | .45            | FMJ         | 230                | 2.4       | II                 | Aramid/UHMWPE<br>w/aramid-based trauma pack |
| 1779'           | .32 Auto       | FMJ         | 73                 | 0.9       | IIIA               | Aramid                                      |
| 3048            | .25 Auto       | FMJ         | 50                 | 2.4       | IIIA               | Aramid/UHMWPE                               |
| 954             | 9 mm           | FMJ         | 124                | 3.7       | II                 | Aramid w/composite plate                    |

Abbreviations: S&W – Smith and Wesson, JHP – Jacketed Hollow Point, FMJ – Full Metal Jacket, FN – Flat Nose, NIJ – National Institute of Justice, UHMWPE – Ultra-High Molecular Weight Polyethylene

^These cases were previously re-created in [20]

^NM07 was shot twice – once in the anterior chest, once more laterally on the rib cage – re-creations of both impacts were performed

A primary difference in the re-creation methodology in this study compared to the previous study was how the moulds of the BFS were made. The Polytek EasyFlo 60 (Bare Metal Foil Company; Farmington, MI) material was still used to create the mould, but the mould captured more volume than just the clay depression to include the plane of the undisturbed portion of the clay and capture the volume of any clay that was expelled from the crater, i.e., the crater lip. To identify the plane of the original clay surface, three metal washers were placed on the surface around the outside of the effective diameter of the crater. The well-mixed, two-part resin was then poured such that the height of the solution was higher than the crater lip. Figure 2 depicts the process of making the mould of the BFS, as well as an example of a casted depression.

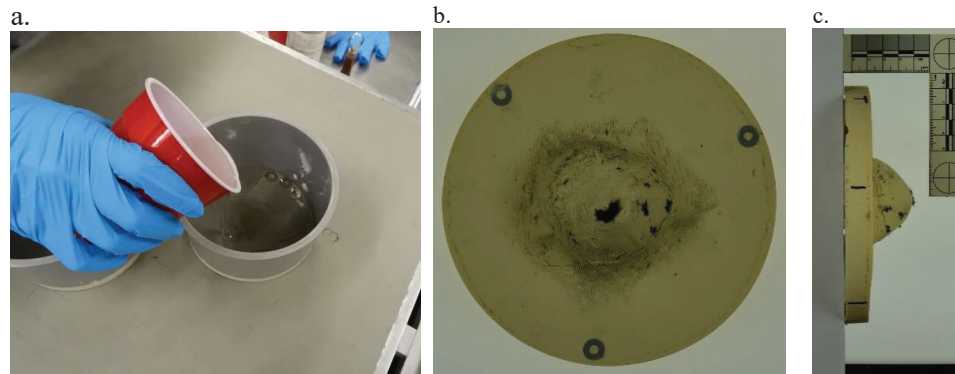


**Figure 2.** a. An example of the casting process to obtain the BFS of the re-created BABT cases. b. An overhead view of a mould of a BABT case created using the methodology described in this study. c. A side-view of the same mould.

All of the moulds available, both previously obtained and newly acquired, were scanned using a CT scanner (GE BrightSpeed Elite CT System, GE® Healthcare). The diameter, depth, volume, and surface area of the deformation profiles were calculated using MATLAB (MATLAB Release 2018a, The MathWorks, Inc., Natick, Massachusetts, United States). For the moulds that were previously obtained, it was assumed that the flat surface of the mould was coincident with the plane of the original clay surface. In the newly-acquired moulds, the centroids of each of the three washers were used to determine the plane of the original clay surface. The diameters, depths, volumes, and surface areas were calculated from that plane as indicated in Figure 3. If the deformation was not symmetric, the average diameter was used for further calculations.

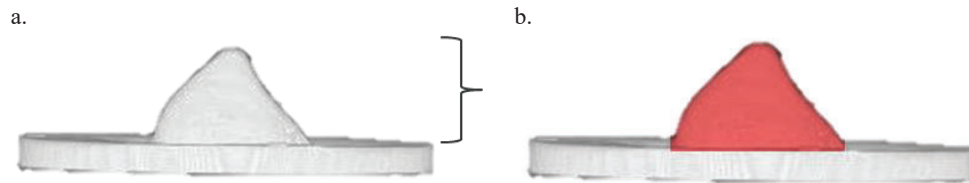


**Figure 3.** a. A depiction of the clay depth measurement from the new moulds obtained in this study. b. An illustration of the portion of the mould evaluated for the volume and surface area. The red-highlighted portion is the region that was analysed.

To analyse the relationship of these backface parameters to injury, the various injuries sustained by the officers had to be consolidated and described using a common scheme. The injuries were initially classified using the Abbreviated Injury Scale (AIS) [21], a commonly-used injury scoring system for traumatic injuries, but the majority of the injuries were considered AIS 1, or minor. This minor category, however, could include superficial bruises as well as fractured ribs. Consequently, similar to the previous study, an additional scoring system was applied to improve the resolution of the minor injuries [2]. Category A included minor skin injuries, while Category B included skin injuries that required wound care and/or internal injuries, e.g., rib fracture, pulmonary contusion, etc.. The categorisation of the skin injuries was confirmed by a board-certified plastic surgeon.

In a similar fashion to other injury relationships, such as the Wayne State Tolerance Curve for head injuries [22] and Bowen's curves for blast lung injuries [23], the likelihood of injury from BABT depends on multiple factors in a non-linear relationship. As in the aforementioned injury curves where the peak acceleration or pressure does not adequately describe the applied loading, the clay depth also does not accurately represent the full extent of the BFS. For this analysis, we assumed that the likelihood of increased injury severity was a function of both the depth and shape of the BFS.

Several empirical observations of how the body responds to impacts, as well as some presumed responses were considered to define the form of this relationship. Previous research has demonstrated that increases in clay depth are associated with an increased risk of injury severity [2, 20], which should be related to the delivered energy. However, other research in injury biomechanics has indicated that the shape of the delivered impact can affect levels of injury [15] and injury patterns [16]. It is expected that a BFS that has a sharper geometry would result in larger stresses and strains around the impact,

increasing the injury risk. Because not all of the clay signatures have simple, spherical geometries, the sharpness cannot be easily calculated, nor does it account for the rest of the surface geometry that would also affect injury risk. To quantify the effect of the shape of the deformation, SA/V of the deformation was calculated. This ratio is problematic, though, if applied across the spectrum of deformation depths, since the ratio decreases as the size increases, regardless of the shape of the deformation. Thankfully, the proportional differences between shapes remain constant for a given characteristic length, BFS depth in this study. To account for this dependence on size, the SA/V of the BFS was compared to the SA/V of a spherical cap with the same depth and diameter as the BFS. A spherical shape was selected for the comparison since that shape demonstrates the lowest SA/V. Figure 4 illustrates the parameters in the surface area and volume calculations of a spherical cap. Using half of the crater diameter for the radius of the base of the cap,  $a$ , and the depth for the height of the cap,  $h$ , the SA/V of the normalising geometry was determined (Equation 1). This form of the SA/V equation could be used since all of the BFS depths in this study were less than the diameters of the BFSs.

$$\frac{SA_{cap}=\pi(a^2+h^2)}{V_{cap}=\frac{1}{6}\pi h(3a^2+h^2)} \quad (1)$$

Equation 2 describes the comparison of the surface area to volume ratio of the BFS with the surface area to volume ratio of the spherical cap. This new ratio increases in value when the BFS becomes more spherical or less sharp of an impact, with a theoretical maximum value of 1.

$$\frac{SA}{V_{norm}} = \frac{\frac{SA_{cap}}{V_{cap}}}{\frac{SA_{BFD}}{V_{BFD}}} \quad (2)$$

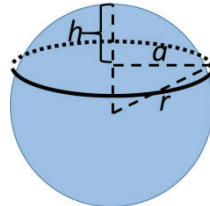


**Figure 4.** The surface area of a spherical cap with a height,  $h$ , equivalent to the clay depth, and a radius of the base of the cap,  $a$ , equivalent to half of the crater diameter was calculated to normalise the SA/V of the BFS.

Assuming the BFSs have primarily convex geometries in the clay, the normalised SA/V of shallower depths does not follow the same trend of describing the sharpness of the BFS for deeper depths. For example, if the depth of the BFS is small and the normalised SA/V is also small, then the surface area of the BFS must be large compared to the volume. Since the depth is small, the geometry would likely describe a relatively broad impact area. A broader impact area would spread the load across a wider area of the body which would decrease the injury risk from this type of impact relative to a more spherical impact. Likewise, when the depths increase and the normalised SA/V is small, the surface area of the BFS must again be large compared to the volume. However, in this scenario, because the depth is deep, the impact area would be narrower and more likely to be injurious. Figure 5 depicts geometries with the same SA/V, but different BFS depths to illustrate this concept.

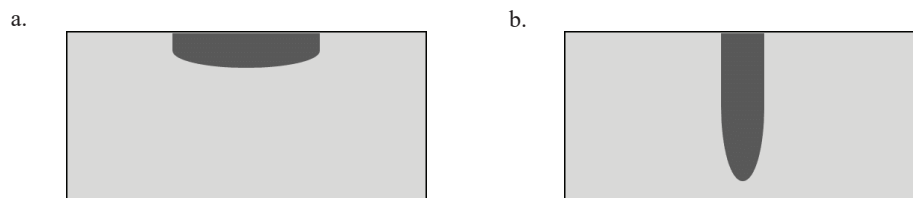


**Figure 5.** Comparison of similar normalised SA/V, but different BFS depths. a. An illustration of a BFS shape with a small depth and normalised SA/V. b. An illustration of a BFS shape with a large depth and small normalised SA/V.

The relationship between BFS depth and the normalised SA/V described in Equation 3 satisfies these changes in injury risk for the different depths and shape factor.

$$depth_{BFS} = D \left( 1 + C \frac{SA^{-b}}{V_{norm}} \right) \quad (3)$$

$D$ ,  $C$  and  $b$  are constants that will be determined from the data collected from the re-created cases. As the geometry of the BFS trends towards a spherical impact, the equation will approach a constant depth,  $D + DC$ . The negative exponential constant describes the effect that in order for BFSs with small volumes, i.e., low energy, to be injurious, the BFS profile must be sharp.

A logistic regression was performed on the BABT cases re-created on clay to express the likelihood of increased injury risk in terms of the BFS depth and normalised SA/V. The logistic regression model was similar to the one described in [22], but the function used as the explanatory variable was as follows in Equation 4:

$$A = \ln \left( D \left( 1 + C \frac{SA^{-b}}{V_{norm}} \right) \right) - \ln(depth_{BFS}) \quad (4)$$

Initial estimates for  $D$ ,  $C$  and  $b$  were made based on the data distribution on the plot of BFS depth and normalised SA/V. The parameter estimates were varied until the model reached a minima with regards to the root-mean squared error and the likelihood-ratio Chi-square test statistic was significant ( $p < 0.05$ ). Generalised  $R^2$  was used to evaluate the goodness-of-fit. The receiver operating curve (ROC) was used to assess the predicted probabilities. A logistic regression was also performed with just the BFS depth for comparison. The logistic regression analyses were carried out using the Logistic platform of the Fit Y by X platform in JMP, version 12.0.1, statistical software (SAS Institute, Inc., Cary, NC, 2015).

### 3. RESULTS

A summary of the 20 cases used in this study are provided in Table 2. An injury classification of B indicates that the survivor had a skin injury that required wound care and/or had an internal injury and A indicates no medical care was required. Some of the values presented in Table 2 differ from earlier published values regarding these cases. The information presented here represents the most-up-to-date and complete data at the time of publication.

**Table 2.** Summary of the BFS in clay for the law enforcement BABT cases

| Case                                 | Injury Classification | Depth (mm) | Diameter (mm) | Volume (mL) | Surface Area (cm <sup>2</sup> ) | Normalised SA/V |
|--------------------------------------|-----------------------|------------|---------------|-------------|---------------------------------|-----------------|
| NM07 <sup>^</sup> ribs <sup>+</sup>  | B                     | 46.09      | 87            | 100         | 62                              | 1.08            |
| 990 <sup>+</sup>                     | B                     | 43.08      | 76            | 94          | 85                              | 0.81            |
| 3029 <sup>+</sup>                    | B                     | 41.77      | 84            | 101         | 99                              | 0.73            |
| 3138 <sup>*</sup>                    | B                     | 39.55      | 82            | 116         | 163                             | 0.53            |
| 1805                                 | B                     | 35.46      | 74            | 93          | 81                              | 0.94            |
| 1753                                 | B                     | 32.75      | 62            | 67          | 76                              | 0.83            |
| 3123 <sup>+</sup>                    | B                     | 32.42      | 67            | 73          | 121                             | 0.55            |
| 2576                                 | B                     | 31.42      | 66            | 52          | 55                              | 0.88            |
| 2840 <sup>+</sup>                    | B                     | 25.26      | 81            | 44          | 54                              | 0.78            |
| 3128                                 | A                     | 29.99      | 67            | 71          | 108                             | 0.63            |
| 1716                                 | A                     | 27.80      | 76            | 65          | 148                             | 0.41            |
| 3166                                 | A                     | 27.68      | 74            | 67          | 77                              | 0.83            |
| NM07 <sup>^</sup> chest <sup>+</sup> | A                     | 27.00      | 93            | 82          | 151                             | 0.49            |
| 3109 <sup>+</sup>                    | A                     | 23.65      | 98            | 75          | 230                             | 0.31            |
| 2914 <sup>+</sup>                    | A                     | 23.51      | 67            | 27          | 28                              | 1.06            |
| 3167 <sup>+</sup>                    | A                     | 21.51      | 75            | 193         | 312                             | 0.69            |
| 3108 <sup>+</sup>                    | A                     | 21.40      | 98            | 51          | 111                             | 0.48            |
| 1779 <sup>+</sup>                    | A                     | 21.01      | 66            | 265         | 409                             | 0.76            |
| 3048                                 | A                     | 12.02      | 47            | 9           | 49                              | 0.37            |
| 954                                  | A                     | 3.38       | 82            | 29          | 222                             | 0.77            |

<sup>+</sup>These cases had an AIS2 injury associated with the BABT event, confirmed via medical records

<sup>\*</sup>The survivor self-reported a pulmonary contusion (AIS2 or 3 depending on degree of lung involvement), no medical records were available to substantiate the diagnosis, the reported skin defect was severe enough to be placed in Injury Classification B

<sup>+</sup>These cases were previously re-created in [20]. The moulds from those experiments were still available so they could be scanned and analysed for this study.

<sup>^</sup>NM07 was shot twice – once in the anterior chest, once more laterally on the rib cage – re-creations of both impacts were performed

The nonlinear model fit for the 50% risk of increased severity of injury is shown in Figure 6. The injury data is plotted along with the fit to show the relationship of the Injury Classification Levels A and B to the fit. The parameters for the regression model are presented in Table 3. Table 3 also summarises the goodness-of-fit of the depth-only and nonlinear regression models. The generalised R<sup>2</sup> is different than the R<sup>2</sup> used in ordinary linear regression, so the values do not represent the proportion of variance, but it still describes a proportion in terms of the log likelihood. A higher generalised R<sup>2</sup> indicates a better fit. The results indicate that the goodness-of-fit and predictive capability of the model improved when using the model that included the shape parameter versus the model that only included depth.

**Table 3.** Model parameters and evaluation

|                                    | DF   | Chi Square | p      | Generalised R <sup>2</sup> | AUC of ROC |
|------------------------------------|------|------------|--------|----------------------------|------------|
| <b>Depth (n=20)</b>                | 1    | 17.70      | <.0001 | 0.64                       | 0.96       |
| <b>Nonlinear Regression (n=20)</b> | 1    | 19.04      | <.0001 | 0.69                       | 0.97       |
| <b>Parameter Estimates</b>         |      |            |        |                            |            |
| <b>D</b>                           | 10.5 |            |        |                            |            |
| <b>C</b>                           | 1.5  |            |        |                            |            |
| <b>-b</b>                          | 0.5  |            |        |                            |            |



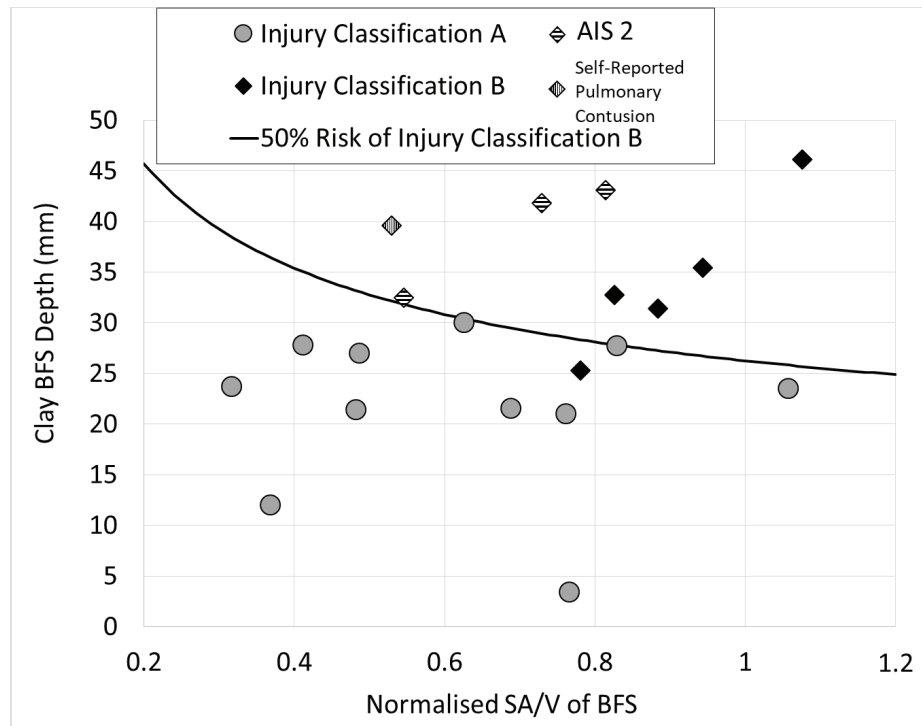


**Figure 6.** Nonlinear regression for increased injury classification using clay BFS depth and a normalised SA/V. The data points associated with AIS 2 injuries and the self-reported pulmonary contusion are highlighted.

#### 4. DISCUSSION

The depth of deformation in clay has been a common method to assess BABT for decades; however, the development of the depth criterion was based on limited data using armour systems and threats that do not represent the current environment. Consequently, there is a lot of uncertainty in what the actual injury risk is for current armour systems and threats at any depth in clay. Although the depth has since been shown to have a moderate correlation to increased injury classification [2], the profile of a BFS at a certain depth can have a wide range of geometries, e.g., larger volumes, sharper shapes, etc., which can also affect the injury risk. Attempts to quantify other BFS metrics in clay have been done, but many of the studies lacked the corresponding injury data to relate the BFS parameters to injury risk [25-27]. This study is unique because it related 20 BFS profiles with associated BABT injuries in humans.

This study confirmed the notion that BFS shape along with depth affected the injury risk from BABT. Shapes that are rounded like a spherical cap have more volume of displaced clay for a particular depth than any other shape. And previous work has shown that the volume of displaced clay is related to the energy of the impact [27]. Therefore, if the volume is related to the amount of energy available to cause injury, spherical BFS shapes could deliver a threshold level of energy to the torso at smaller clay BFS depths, as indicated in Figure 6. Conversely, to reach the same energy threshold – volume of displaced clay – for sharper geometries, the clay deformation would have to be deeper. In other words, the injury relationship to geometric features of the BFS derived in this study was actually an injury assessment tool related to energy, and it has been shown that metrics associated with energy were better predictors of injury to the thorax, especially for high velocity, low mass impacts, like BABT [2, 28-29].

The fit to the nonlinear regression identified in this study describes the 50% risk of having an injury in Injury Classification B, i.e., a skin injury that required wound care and/or had an internal injury. Therefore, the injury risk described is for relatively mild injuries. However, it is expected that the general trend of the injury risk being related to the depth and shape of the BFS would be the same for serious localised injuries. The cases that had moderate injuries, AIS 2, had associated BFS depths that were generally deeper than the AIS 1 injuries. These moderate injury cases were also associated with BFSs that trended away from a spherical shape. Investigation of these profiles demonstrated irregular geometries (Figure 1b and 7), such that there were localised areas that could have relatively high impact



energy densities, providing more evidence that injury is associated with not just energy, but how it is delivered.



**Figure 7.** An example of an irregular geometry that has a region that could impact the body with a relatively high energy density.

The small number of primarily soft armour cases in this study, the unique and complex nature of each case, and the limited range of injury severities reduces the confidence in the exact probability of injury estimates of interest to armour designers and evaluators, but this analysis sets a foundation to build upon to relate the static clay BFS to the energy available to cause injury. In particular, there are uncertainties into whether this technique would apply to non-normal angles of trajectory or hard armour, as those scenarios were not directly studied, but are of interest to the community. Non-normal impacts have several aspects to consider before a robust relationship between BFS and injury can be made: how the clay deformation is affected by impact angle, and how the angle is presented to the body. For example, if the impact angle of  $45^\circ$  impacted the subject on the left side of the chest such that the angle was also pointing to the left, the amount of energy deposited into the body would be less than if that same angle was pointing to the right, potentially affecting injury risk. With regards to hard armor, one of the significant differences between soft and hard armour impacts is the potential for increased backface velocities for hard armour. Even though the BFS is a function of backface velocity, the BFS cannot capture, for similar deformation profiles, the rates of deformation. Previous work has indicated that the best metric for predicting increased injury was the Blunt Criterion (BC) [2], a metric that requires measuring or calculating the backface velocity of the armour, which is difficult and costly. As technology improves, it is likely it will be trivial to measure the backface velocity in the future; however, in the meantime, a metric that involves measuring the static BFS profile could be more easily implemented and may have a better relationship with injury than the current metric of BFS depth. More work needs to be done to investigate to what degree this rate parameter and non-normal impacts affect injury risk for various BABT impact conditions.

Clay is still often used to assess BABT. While alternative tools and devices have been and are being designed to improve the ability to evaluate the injury risk from BABT events, adoption of these devices has not occurred or will not likely occur quickly. Therefore, improving the metrics using the current clay methodology can more quickly address the immediate need to evaluate and optimise newer and lightweight armour systems.

## 5. CONCLUSION

This study has determined a relationship between the shape of the backface deformation in clay to increased injury risk from 20 re-created BABT impact events. As clay is still the most widely-used method to assess BABT, identifying a metric that can improve the ability to assess injury risk using the depression left in clay is desired. The depth and shape of the backface deformation in clay is associated with the energy and energy density of the impact, two parameters that have been shown to have a good relationship to injuries for high-rate, low-mass impacts, like BABT. The dataset for this analysis is currently limited, but the relationship exhibits potential for an improved metric that can be easily implemented into current testing methodologies and facilities.

## Acknowledgments

This project was supported, in part, by Award No. 2011-IJ-CX-K006, awarded by the National Institute of Justice, Office of Justice Programs, U.S. Department of Justice, and Cooperative Agreement No. W911NF-17-2-0072 with the U.S. Army Research Laboratory. The opinions, findings or conclusions or recommendations expressed in this publication are those of the authors and do not necessarily reflect those of the Department of Justice or the Department of Defense. The authors would like to thank, first and foremost, all of the survivors who consented to participate in the study. We would also like to thank Erika Matheis, Rodrigo Villalta, Katherine Hewins, Nick Rowley, John Cavanaugh, and the Wayne State University Ballistics Injury Laboratory group.

## References

- [1] National Institute of Justice. Ballistic Resistance of Body Armor, NIJ Standard - 0101.06. (Available at: National Criminal Justice Reference System <https://www.ncjrs.gov/pdffiles1/nij/223054.pdf>, 2008, accessed 19 August 2011).
- [2] Rafaels K.A., Loftis K.L., and Bir C.A., Can Clay Tell Us More Than Deformation?, Proceedings of the Personal Armour Systems Symposium, Washington D.C., USA, Oct. 1-5, 2018.
- [3] Nader J., and Dagher H., Exp Tech, 2011; 35(2); 55-60.
- [4] O'Masta MR, Compton BG, Gamble EA, Zok FW, Deshpande VS and Wadley HNG, Int. J. Impact Eng., 2015; 86, 131-144.
- [5] Bass C.R., Salzar R.S., Lucas S.R., Davis M., Donnellan L., Folk B., Sanderson E., and Waclawik S., Int J Occup Saf Ergon, 2006; 12(4); 429-442.
- [6] Amarilio I.B., Benes D., Asaf Z., Ya'akobovich A., Shmulevich I., Mouradjian A., Wolf A., Grunner S., and Kluger Y., Proceedings of the Personal Armour Systems Symposium, Nuremburg, Germany, Sept. 17-21, 2012.
- [7] Stuivinga M., Carton E.P., Verbeek, H.J., and van Bree J.L.M.J., Proceedings of the Personal Armour Systems Symposium, Nuremburg, Germany, Sept. 17-21, 2012.
- [8] Broos J.P.F., van der Jagt-Deutekom, M., Halls V.A., and Zheng J.Q., Proceedings of the Personal Armour Systems Symposium, Nuremburg, Germany, Sept. 17-21, 2012.
- [9] Metker L.W., Prather R.N., and Johnson E.M., A Method for Determining Backface Signatures of Soft Body Armors, U.S. Army Edgewood Arsenal, Technical Report, TR-75029, 1975.
- [10] Mauzac O., Paquier C., Debord E., Barbillon F., Mabire P., and Jacquet J.F., Proceedings of the Personal Armour Systems Symposium, Quebec City, Canada, Sept. 14-17, 2010.
- [11] Goode T., Shoemaker G., Schultz S., Peters K., and Pnakow M., Compos. Struct., 2019; 220, 687-698.
- [12] Hinsley DE, Tam W, and Evison D, Behind Armour Blunt Trauma to the Thorax – Physical and Biological Models, Proceedings of the Personal Armour Systems Symposium, The Hague, Netherlands, Nov 18-22, 2002.
- [13] Bourget, D, B Anctil, D Doman, and D Cronin, Development of a Surrogate Thorax for BABT Studies, Proceedings of the Personal Armour Systems Symposium, The Hague, Netherlands, Nov 18-22, 2002.
- [14] Arborelius UP, Tryberg A, Gustavsson J, Malm E, Gryth D, Olsson LG, Skoglund M, Rocksen D, Proceedings of the Personal Armour Systems Symposium, Nuremberg, Germany Sept. 17-21, 2012, pp. 305-314.
- [15] Cronin DS, J Biomechanics, 2007; Volume 40, Supplement 2; S48.
- [16] Crandall JR, Bass CR, Duma SM, and Kuppia S. J Passeng Cars, 1998; Volume 107; 1154-1161.
- [17] Shergold O and Fleck N. Proc R Soc Lond A, 2004; 460; 3037-3058.
- [18] Shergold OA and Fleck NA. J Biomech Eng, 2005; 127: 838-848.
- [19] Hewins K, Anctil B, Stojisih S, and Bir C, Ballistic Blunt Trauma Assessment Methodology Validation, Proceedings of the Personal Armour Systems Symposium, Nuremburg, Germany, Sept 18-21, 2012; pp. 315-323.
- [20] Bir C, Lance R, Stojisih-Sherman S, and Cavanaugh J, Behind Armor Blunt Trauma: Recreation of Field Cases for the Assessment of Backface Signature Testing, Proceedings of the 30<sup>th</sup> International Symposium on Ballistics, Long Beach, CA, USA, Sept. 11-15, 2017.
- [21] Association for the Advancement of Automotive Medicine. Abbreviated Injury Scale—2005 Update 2008. Chicago, IL.; 2008.
- [22] Lissner HR, Lebow M, and Evans FG, Surg Gynecol Obstet, 1960; 111; 329-338.
- [23] Bowen IG, Fletcher ER, and Richmond DR, Estimate of Man's Tolerance to the Direct Effects of Air Blast, Defense Atomic Support Agency, Report, DASA-2113, 1968.
- [24] Bass CR, Rafaels KA, Salzar RS, J Trauma, 2008; 65; 604-615.

- [25] Murphy MJ, Survey of the Influence of Velocity and Material Properties on the Projectile Energy/Target Hole Volume Relationship, Proceedings of the 10<sup>th</sup> International Symposium on Ballistics, San Diego, CA, USA, 1987.
- [26] Broos JPF, vsn der Jagt-Deutekom M, Halls VA, and Zheng JQ, Separation Between Armour and Clay Backing during Projectile Impact, Proceedings of the Personal Armour Systems Symposium, Nuremburg, Germany, Sept 18-21, 2012.
- [27] Bevan M and Luong Q, Correlation between Projectile Kinetic Energy and Displaced Clay Volume for Three Classes of Armour, Proceedings of the Personal Armour Systems Symposium, Washington, D.C., USA, Oct. 1-5, 2018.
- [28] Sturdivan LM, Viano DC, and Champion HR, J Trauma, 2004; Volume 56; 651-663.
- [29] Viano DC and Lau IV, J Biomechanics, 1988; Volume 21; 387-399.